

# UC Irvine

## UC Irvine Previously Published Works

### Title

Entorhinal-Hippocampal Circuit Integrity Is Related to Mnemonic Discrimination and Amyloid- $\beta$  Pathology in Older Adults.

### Permalink

<https://escholarship.org/uc/item/4266572j>

### Journal

Journal of Neuroscience, 42(46)

### ISSN

0270-6474

### Authors

Adams, Jenna N

Kim, Soyun

Rizvi, Batool

et al.

### Publication Date


2022-11-16

### DOI

10.1523/jneurosci.1165-22.2022

Peer reviewed

# Entorhinal–Hippocampal Circuit Integrity Is Related to Mnemonic Discrimination and Amyloid- $\beta$ Pathology in Older Adults

Jenna N. Adams,<sup>1,2</sup> Soyun Kim,<sup>1,2</sup> Batool Rizvi,<sup>1,2</sup> Mithra Sathishkumar,<sup>1,2</sup> Lisa Taylor,<sup>3</sup> Alyssa L. Harris,<sup>1,2</sup> Abanoub Mikhail,<sup>1,2</sup> David B. Keator,<sup>3</sup> Liv McMillan,<sup>1,2</sup> and  Michael A. Yassa<sup>1,2,3</sup>

<sup>1</sup>Department of Neurobiology and Behavior, University of California, Irvine, Irvine, California 92697, <sup>2</sup>Center for the Neurobiology of Learning and Memory, University of California, Irvine, Irvine, California 92697, and <sup>3</sup>Department of Psychiatry and Human Behavior, University of California, Irvine, Irvine, California 92697

Mnemonic discrimination, a cognitive process that relies on hippocampal pattern separation, is one of the first memory domains to decline in aging and preclinical Alzheimer's disease. We tested whether functional connectivity (FC) within the entorhinal–hippocampal circuit, measured with high-resolution resting state fMRI, is associated with mnemonic discrimination and amyloid- $\beta$  ( $A\beta$ ) pathology in a sample of 64 cognitively normal human older adults (mean age,  $71.3 \pm 6.4$  years; 67% female). FC was measured between entorhinal–hippocampal circuit nodes with known anatomical connectivity, as well as within cortical memory networks.  $A\beta$  pathology was measured with <sup>18</sup>F-florbetapir-PET, and neurodegeneration was assessed with subregional volume from structural MRI. Participants performed both object and spatial versions of a mnemonic discrimination task outside of the scanner and were classified into low-performing and high-performing groups on each task using a median split. Low object mnemonic discrimination performance was specifically associated with increased FC between anterolateral entorhinal cortex (aLEC) and dentate gyrus (DG)/CA3, supporting the importance of this connection to object memory. This hyperconnectivity between aLEC and DG/CA3 was related to  $A\beta$  pathology and decreased entorhinal cortex volume. In contrast, spatial mnemonic discrimination was not associated with altered FC.  $A\beta$  was further associated with dysfunction within hippocampal subfields, particularly with decreased FC between CA1 and subiculum as well as reduced volume in these regions. Our findings suggest that  $A\beta$  may indirectly lead to memory impairment through entorhinal–hippocampal circuit dysfunction and neurodegeneration and provide a mechanism for increased vulnerability of object mnemonic discrimination.

**Key words:** aging; Alzheimer's disease; amyloid- $\beta$ ; functional connectivity; hippocampus; memory

## Significance Statement

Mnemonic discrimination is a critical episodic memory process that is performed in the dentate gyrus (DG) and CA3 subfield of the hippocampus, relying on input from entorhinal cortex. Mnemonic discrimination is particularly vulnerable to decline in older adults; however, the mechanisms behind this vulnerability are still unknown. We demonstrate that object mnemonic discrimination impairment is related to hyperconnectivity between the anterolateral entorhinal cortex and DG/CA3. This hyperconnectivity was associated with amyloid- $\beta$  pathology and neurodegeneration in entorhinal cortex, suggesting aberrantly increased network activity is a pathological process. Our findings provide a mechanistic explanation of the vulnerability of object compared to spatial mnemonic discrimination in older adults and has translational implications for choice of outcome measures in clinical trials for Alzheimer's disease.

Received June 14, 2022; revised Sep. 30, 2022; accepted Oct. 4, 2022.

Author contributions: J.N.A. and M.A.Y. designed research; J.N.A., A.L.H., A.M., D.B.K., L.M., and M.A.Y. performed research; J.N.A., S.K., B.R., M.S., L.T., A.L.H., and D.B.K. analyzed data; J.N.A. wrote the paper.

This research was supported by the National Institute on Aging (Grant R01-AG-053555, to M.A.Y.; Grant F32-AG-074621, to J.N.A.) and the Alzheimer's Disease Research Center at the University of California, Irvine (Grant P50-AG-016573).

M.A.Y. is Co-founder and Chief Scientific Officer of Augnition Labs, LLC. The authors declare no other competing financial interests.

Correspondence should be addressed to Jenna N. Adams at jnadams@uci.edu or Michael A. Yassa at myassa@uci.edu.

<https://doi.org/10.1523/JNEUROSCI.1165-22.2022>

Copyright © 2022 the authors

## Introduction

Episodic memory decline is a hallmark feature of aging and Alzheimer's disease (AD). Mnemonic discrimination, a process that supports episodic memory, is particularly vulnerable to decline in older adults (Leal and Yassa, 2018). Mnemonic discrimination relies on pattern separation, the ability to differentiate similar memories into distinct, orthogonalized neural representations, which reduces interference and enables the encoding of highly similar experiences as unique episodes (Yassa and Stark, 2011). This neural computation requires intact processing in the

dentate gyrus (DG) and CA3 subfield of the hippocampus and is dependent on direct input from the entorhinal cortex via the perforant pathway (Wilson et al., 2006; Witter, 2007; Yassa and Stark, 2011; Berron et al., 2016).

In aging, reduced inhibitory control in DG/CA3 may lead to CA3 hyperactivation, driven by recurrent collaterals in this network (Wilson et al., 2006), resulting in a shift in computational balance toward pattern completion, or the retrieval of existing representations when prompted with partial cues (Wilson et al., 2005; Leal and Yassa, 2018). Previous studies have demonstrated that DG/CA3 hyperactivation is associated with worse mnemonic discrimination performance (Yassa et al., 2010, 2011b; Bakker et al., 2012), suggesting it is an index of dysfunction. In older adults, mnemonic discrimination of object stimuli declines more sharply compared with spatial stimuli (Reagh et al., 2016; Güsten et al., 2021). This differential vulnerability may result from distinct information processing pathways within the entorhinal cortex (EC), in which the anterolateral subregion of the EC (aLEC) and the posteromedial subregion of the EC (pmEC) preferentially process object and spatial information, respectively (Knierim et al., 2014; Reagh and Yassa, 2014; Maass et al., 2015; Berron et al., 2018).

The development of amyloid- $\beta$  ( $A\beta$ ) and hyperphosphorylated tau, the pathologic proteins characteristic of AD, may underlie impaired mnemonic discrimination. The aLEC is among the first cortical regions to develop tau pathology, which specifically targets the layer II cells that project to DG/CA3 as the perforant path (Braak and Braak, 1985, 1991).  $A\beta$  pathology can cause aberrant neural activity in the medial temporal lobe (Busche et al., 2008; Palop and Mucke, 2010; Mormino et al., 2012; Huijbers et al., 2014, 2015) and promote the development of tau in entorhinal cortex (Sanchez et al., 2021; Adams et al., 2022). Together, these two pathologies likely impede normal function of the entorhinal–hippocampal circuit, impairing mnemonic discrimination, with the object domain particularly vulnerable because of earlier susceptibility of aLEC to pathology.

Because Alzheimer's pathology begins to develop while older adults are still cognitively normal (Jack et al., 2010), it is critical to assess how the emergence of this pathology may lead to entorhinal–hippocampal circuit dysfunction and mnemonic discrimination deficits. Previous studies relating Alzheimer's pathology to medial temporal lobe function during pattern separation have focused on measures reflecting the whole hippocampus and task-based functional activation (Marks et al., 2017; Berron et al., 2019; Maass et al., 2019). Because input from entorhinal cortex to DG/CA3 is critical for pattern separation, assessing functional connectivity (FC) between these subregions may provide sensitive information about the integrity of this circuit.

The goal of the current study was to determine whether Alzheimer's pathology leads to altered FC within the entorhinal–hippocampal circuit, resulting in impaired mnemonic discrimination. To test this, we conducted high-resolution resting state functional MRI on nondemented older adults who also performed object and spatial versions of a mnemonic discrimination task. Because of distinct information processing pathways, we hypothesized that impaired object mnemonic discrimination would be associated with altered FC between aLEC and DG/CA3, while impaired spatial mnemonic discrimination would be related to altered FC between pmEC and DG/CA3. We next tested whether  $A\beta$  pathology would be associated with altered FC between entorhinal cortex and DG/CA3, providing a potential mechanism for decline in mnemonic discrimination, as well

as further FC disruption between hippocampal subfields due to its potential widespread impact on the circuit. Finally, we tested whether neurodegeneration within the entorhinal–hippocampal circuit and FC within cortical memory networks were related to mnemonic discrimination and  $A\beta$  pathology.

## Materials and Methods

### Participants

Cognitively normal older adults  $\geq 60$  years of age either sex from the Biomarker Exploration in Aging, Cognition, and Neurodegeneration (BEACoN) study (Principal Investigator, M.A.Y.; National Institute on Aging Grant R01-AG-053555) with high-resolution resting state fMRI ( $N = 89$ ) were selected for analysis. After exclusion for fMRI data quality (i.e., signal dropout, field of view, motion; see below for details), data from 64 participants were analyzed. Inclusion criteria for BEACoN includes age  $\geq 60$  years, performance on cognitive assessments within age-adjusted normal range (within 1.5 SDs), no major health problems, comorbid neurologic disease, or significant psychiatric disorders, no use of medication for anxiety or depression or illicit drugs, and no MRI or PET contraindications. All participants provided written informed consent in accordance with the Institutional Review Board of the University of California, Irvine.

### Cognitive data

**Mnemonic discrimination task.** Participants performed a mnemonic discrimination task (MDT) with both an object version (MDTO) and a spatial version (MDTS; Fig. 1A), similar to previously described versions (Reagh et al., 2018). Briefly, each task consisted of a study phase, where participants are asked to make “indoor/outdoor” judgements about each stimulus (presented for 2 s; interstimulus interval, 0.5 s). In the object version, each object is presented at the center of the screen, while in the spatial version, each object is presented in a random grid position within the screen. After the study phase, participants complete a test phase. In the object version, the test phase consists of identical repeats of object stimuli (targets; correct response, “old”) and lure stimuli (correct response, “new”), which have either low or high visual similarity to the original object. In the spatial version, participants are tested on the spatial position of each object, with targets in the exact same location (correct response, “same”), and lure stimuli (correct response, “different”) with either low similarity (presented within a different quadrant of the grid) or high similarity (presented within a different position within the same quadrant) to the original target location. Novel foil items (i.e., brand new items; correct response, “new”) are also shown during the test phase of both versions. Participants were allowed 2 s to make a response before the next stimulus appeared. Each participant saw a unique order of stimuli for each phase.

As with all of our prior work using the MDT tasks, we calculated the response bias-corrected lure discrimination index (LDI) quantified as  $p(\text{“New or Different”} \mid \text{Lure}) - p(\text{“New or Different”} \mid \text{Target})$  for the object and spatial task versions separately. We also calculated LDI specifically for highly similar object and spatial lures. We focused our analyses on the highly similar lure trials to tax pattern separation performance but also replicated analyses with all trial types combined. In line with previous human (Stark et al., 2010, 2013; Reagh et al., 2014) and rodent (Gallagher et al., 2003, 2006; Wilson et al., 2006) work, we classified participants into low-performing and high-performing groups (analogous to “aged-impaired” and “aged-unimpaired” groups in these studies). Groups were divided by performing a median split of high-similarity LDI score on the object (median = 0.185; low, MDTO–; high, MDTO+) and spatial (median = 0.21; low, MDTS–; high, MDTS+) trials, separately. Figure 1B shows a visualization of distributions for object and spatial MDT performance and the median split cut points applied.

**Neuropsychological assessment.** Participants also performed standard neuropsychological assessments, including the Rey Auditory Verbal Learning Test (RAVLT; Rey, 1958) and the Mini-Mental State Examination (MMSE; Folstein et al., 1975). The delayed recall measure of the RAVLT (A7), in which participants are assessed on free recall of the list of words after a 20 min delay, was

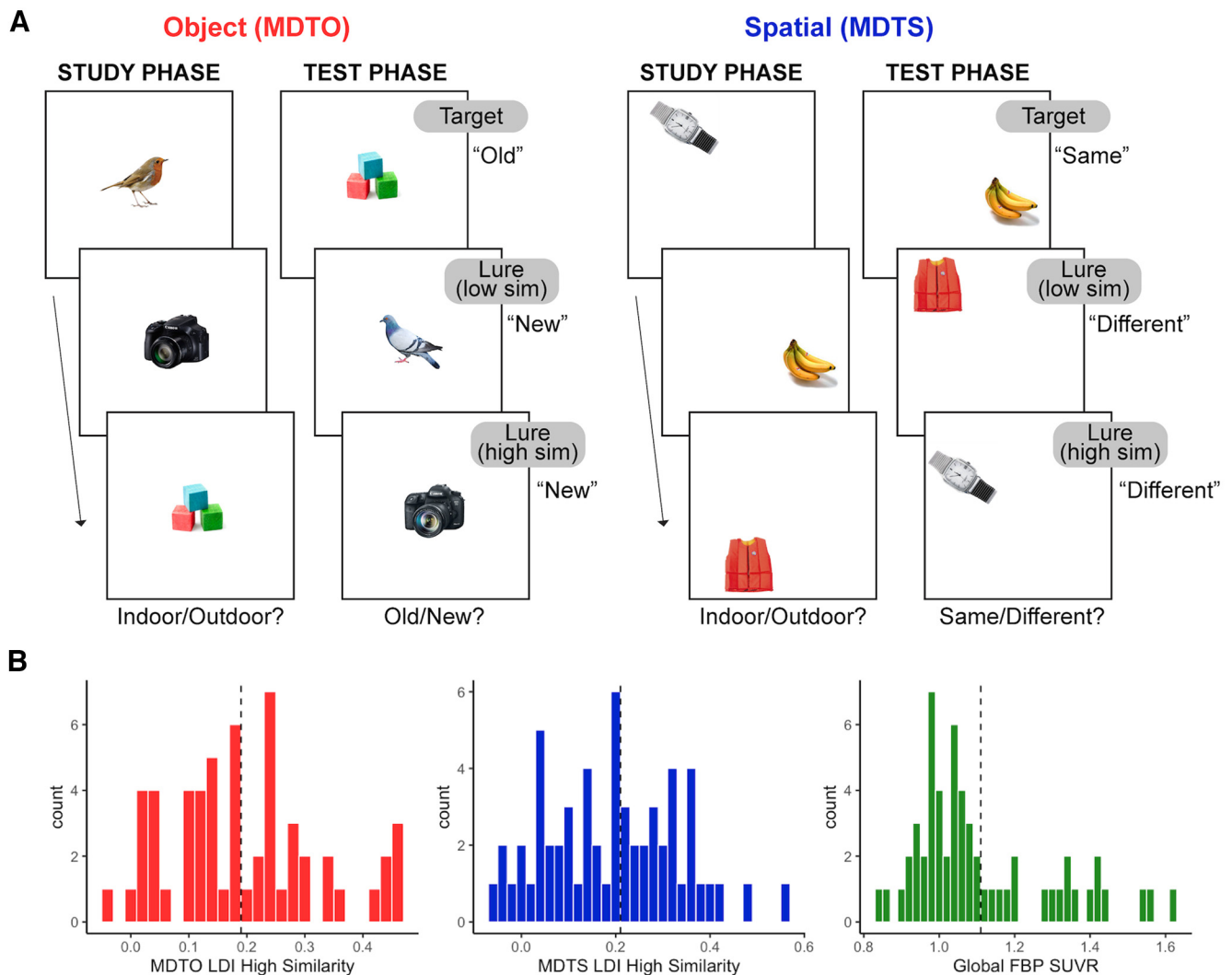


**Figure 1.** Schematic of the mnemonic discrimination task and distribution of performance and  $A\beta$  pathology. **A**, Older adult participants completed both object (MDTO) and spatial (MDTS) versions of a mnemonic discrimination task. During the study phase, participants indicated whether each stimulus was more likely to be found indoors or outdoors. In the test phase, participants indicated whether each stimulus was old (target) or new (lure) in the MDTO and same (target) or different (lure) in the MDTS. In the MDTO, lure stimuli consisted of variations to the object stimulus itself, while in the MDTS, lure stimuli were in a different spatial position on a grid. Lure stimuli in both tasks could be considered low similarity, where the differences were more readily detectable, or high similarity, where the changes were more subtle. Novel foil items (i.e., brand new items: new) are also shown during the test phase but are not depicted in the figure. We defined high and low performers on each task based on the lure discrimination index (LDI) [ $p(\text{"New or Different"} | \text{Lure}) - p(\text{"New or Different"} | \text{Target})$ ] computed from the highly similar lure stimuli, which maximally tax pattern separation mechanisms. **B**, Distribution of performance on the MDTO and MDTS for high-similarity trial types. The median value of each task (dotted line) was used as a cut point to divide older adults into low-performing and high-performing groups on each measure. Older adults were divided into  $A\beta^-$  and  $A\beta^+$  groups based on global  $^{18}\text{F}$ -florbetapir-PET (FBP) PET SUVR, with a cut point of 1.11 SUVR (dotted line) used as a cut point.

used for control analyses testing general episodic memory. Participants were similarly grouped into low and high performers with a median split (median = 11; low, RAVLT-; high, RAVLT+).

#### MRI acquisition

All participants received structural and resting state functional MRI at University of California, Irvine on a 3T Prisma scanner (Siemens Medical System) equipped with a 32-channel head coil. A whole-brain, high-resolution T1-weighted volumetric MPRAGE (magnetization-prepared rapid acquisition gradient echo) image was acquired for structural analyses (voxel size,  $0.8 \text{ mm}^3$  resolution; TR, 2300 ms; TE, 2.38 ms; TI, 902 ms; flip angle,  $8^\circ$ ; 240 slices acquired sagittally). High-resolution T2\*-weighted echoplanar images were acquired to assess FC (voxel size,  $1.8 \text{ mm}^3$  resolution; TR, 2500; TE, 26 ms; flip angle,  $70^\circ$ ; 39 slices; right to left phase encode; partial acquisition covering temporal lobe, 84 volumes). During acquisition, participants were instructed to remain awake and focus on a fixation cross on the screen. High-resolution 3D T2-weighted turbo spin echo images were

acquired in oblique coronal orientation (voxel size,  $0.4 \times 0.4 \text{ mm}$  in-plane resolution; slice thickness, 2 mm; TR, 5000 ms; TE = 84 ms; 23 slices) for hippocampal segmentation and volumetry.

#### Structural MRI processing

Structural T1 images were used for coregistration of both MRI and PET, and for segmentation of medial temporal subregions. T1 images were processed with SPM12 (Wellcome Trust Center) and segmented into gray, white, and CSF compartments. T1 images were then skull stripped and warped to a study-specific template using Advanced Normalization Tools (ANTs; Tustison et al., 2021). T1 images were also processed with FreeSurfer version 6.0 (Fischl, 2012) to obtain a native space regions of interest (ROIs) for PET quantification.

To obtain measures of medial temporal lobe subregional volumes, both T1 and T2 structural images were processed using Automated Segmentation of Hippocampal Subfield (ASHS) software (Yushkevich et al., 2015). Segmentations were visually quality checked by trained researchers, and all passed inspection. Volumes of the entorhinal cortex,



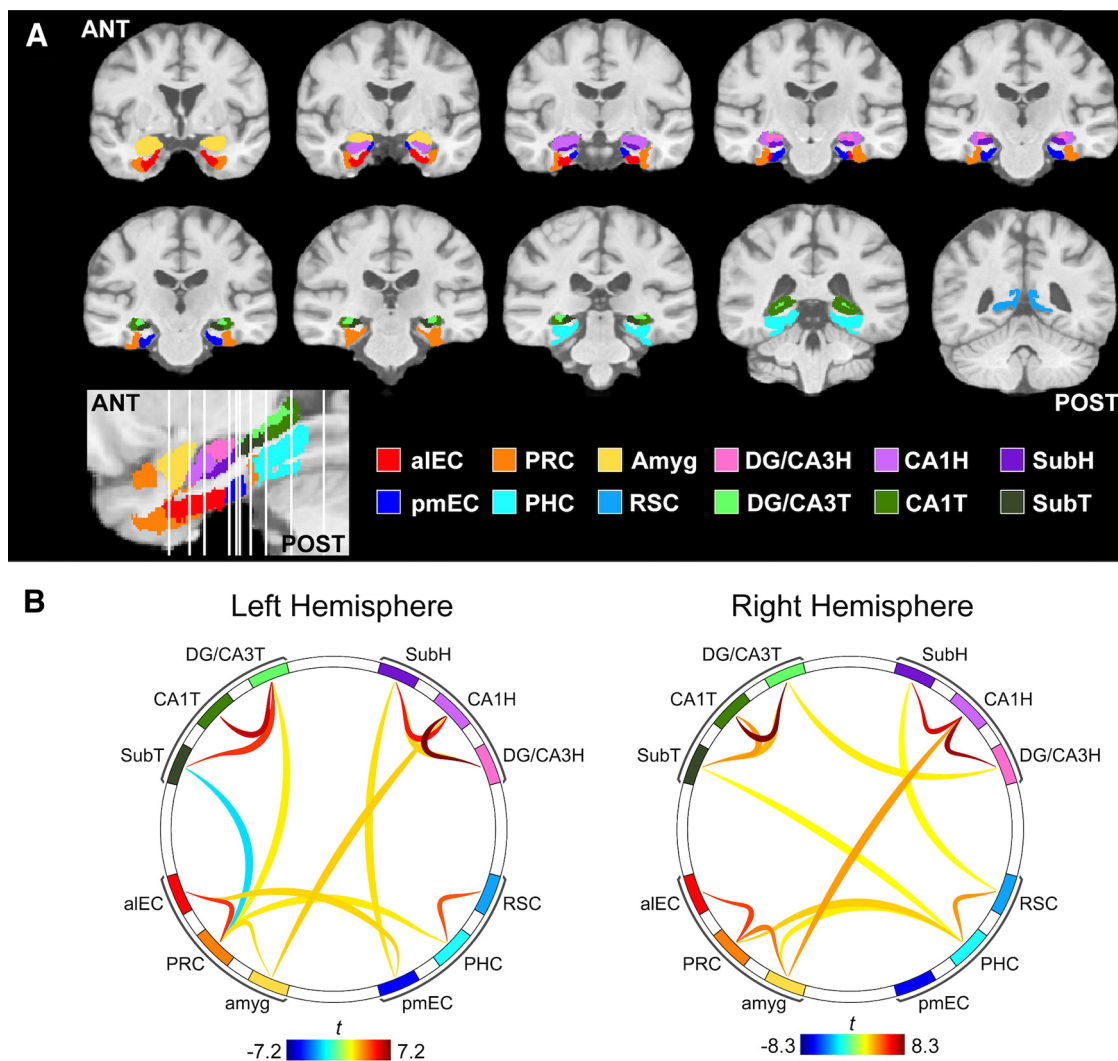


**Figure 2.** Functional connectivity (FC) methods and group-level results. We measured FC between ROIs based on a high-resolution study-specific atlas, which spanned the medial temporal lobes and related regions. **A**, ROIs included the anterior-temporal cortical network (anterolateral entorhinal cortex, aIEC; perirhinal cortex, PRC; amygdala, amyg), posterior-medial network (posteromedial entorhinal cortex, pmEC; parahippocampal cortex, PHC; retrosplenial cortex, RSC), as well as hippocampal subfields within the head (H) and tail (T) segments (dentate gyrus/CA3, DG/CA3; CA1; subiculum, Sub). **B**, Seed-to-seed FC was performed using semipartial correlations. Group-level results were thresholded using a connection threshold of  $p < 0.05$   $p$ -uncorrected and an ROI-level threshold of  $p < 0.05$   $p$ -FDR corrected. FC was similar between hemispheres and predominantly occurred within networks.

DG, CA3, CA1, and subiculum (Sub) were used for analyses and normalized by total intracranial volume (TIV) estimates derived from ANTs.

#### Resting state functional MRI processing

Resting state fMRI data were preprocessed with SPM12 using a standard pipeline including slice time correction, realignment, and coregistration to the T1 structural image. No spatial smoothing was performed to maintain the high resolution of the images and enable more accurate quantification of signal within spatially adjacent subregions. Functional images were warped to the study-specific template with ANTs, applying the transformation parameters derived from structural warping.

**ROIs.** ROIs were defined using an in-house atlas of the temporal lobe and related regions, described in detail previously (Yassa et al., 2011a; Reagh and Yassa, 2014; Reagh et al., 2018). Briefly, the segmentation of hippocampal subfields (Yuskevich et al., 2015; Wisse et al., 2017), entorhinal subregions (for functionally defined ROIs, see Maass et al., 2015; Navarro Schröder et al., 2015; for a full description, see Reagh et al., 2018), and cortical temporal regions (Insausti et al., 1998) was performed in accordance with standardized reliable protocols. The analysis included the following regions: aIEC, pmEC, perirhinal cortex (PRC), parahippocampal cortex (PHC), amygdala (amyg), retrosplenial cortex (RSC), head of DG/CA3 (DG/CA3H) and tail of DG/CA3 (DG/CA3T),

head of CA1 (CA1H) and tail of CA1 (CA1T), and head of Sub (SubH) and tail of Sub (SubT), bilaterally. ROIs across 10 coronal slices spanning the length of the ROI atlas are depicted in Figure 2A.

To ensure that all ROIs had reliable signals because of the possibility of signal dropout in medial temporal lobe, we performed strict thresholding and exclusion of low signal. For each participant, the mean signal across the gray matter was quantified, and voxels with  $<25\%$  of the mean gray matter signal were removed. Participants with  $<50\%$  of any ROI remaining were excluded from subsequent analyses because of lack of data, resulting in the exclusion of 13 participants. Two additional participants were excluded because of the partial acquisition field of view not including the full extent of the medial temporal lobe.

**Denoising.** Resting state fMRI data were optimized for FC analyses using the CONN toolbox (version 20; Whitfield-Gabrieli and Nieto-Castanon, 2012) implemented in MATLAB version 2019b (MathWorks). Outlier volumes were detected using Artifact Detection Tools implemented within CONN using conservative threshold of motion  $>0.5$  mm/TR and a global intensity  $z$  score of 3. Ten subjects were flagged for  $>20\%$  volumes detected as outliers and were removed from further analyses (Adams et al., 2019; Maass et al., 2019). Denoising was then performed, including six realignment parameters and their first-order derivatives (translations and rotations), spike regressors generated from outlier

detection (Lemieux et al., 2007; Power et al., 2015), anatomic CompCor (first five components of time series signal from white matter and CSF; Behzadi et al., 2007), bandpass filter (0.008–0.1 Hz), and linear detrending applied to the residual time series.

**Functional connectivity analysis.** Using CONN, denoised time series were extracted from each ROI, and semipartial correlations were used to perform ROI-to-ROI FC analyses. Semipartial correlations were chosen to control for any signal bleed in between spatially adjacent ROIs (Adams et al., 2019; Dalton et al., 2019). FC strength (Fisher's  $r$  to  $z$ -transformed correlation coefficient) was extracted for each ROI pair. Because we did not have specific hypotheses about hemispheric lateralization, and to reduce the number of statistical comparisons, we averaged FC strength between left and right ROI pairs for all analyses.

Second-level analyses were conducted in CONN. To determine patterns of group-level FC, we performed a between-subjects contrast using a one-sample  $t$  test (two-tailed) for all seeds within each hemisphere (Fig. 2B). Significant connections were determined with a connection-level threshold of  $p < 0.05$   $p$ -uncorrected (two-sided) and an ROI-level threshold of  $p < 0.05$   $p$ -false discovery rate (FDR) corrected, which corrects for multiple comparisons by using a multivariate pattern analysis omnibus test to characterize the strength of all connections from each ROI (Whitfield-Gabrieli and Nieto-Castanon, 2012).

### *A $\beta$ pet*

To quantify  $A\beta$  pathology, participants received  $^{18}\text{F}$ -florbetapir (FBP) PET performed on an ECAT High-Resolution Research Tomograph (CTI/Siemens) at the Campus Center for Neuroimaging. Ten millicurie of tracer was injected, and four 5 min frames were collected between 50 and 70 min post-injection. FBP data were reconstructed with attenuation correction, scatter correction, and 2 mm<sup>3</sup> Gaussian smoothing. FBP images were then realigned, coregistered to the T1 MRI, and normalized by a whole cerebellum reference region to produce standardized uptake value ratio (SUVR) images. Additional 6 mm<sup>3</sup> Gaussian smoothing was then applied to achieve an effective resolution of 8 mm<sup>3</sup>. The mean SUVR of a previously validated cortical composite region was quantified as a measure of global  $A\beta$  (Fig. 1B, distribution of global  $^{18}\text{F}$ -FBP SUVR), and  $A\beta+$  status was determined using a threshold of  $>1.11$  SUVR (Landau et al., 2012).

### *Experimental design and statistical analyses*

All statistical analyses were performed using jamovi version 1.6 (<https://www.jamovi.org>) and RStudio version 1.4. FC differences across groups were assessed with repeated-measures ANCOVAs, with FC (FC between ROI pairs) as a within-subjects factor, group based on performance or  $A\beta$  status (e.g., MDTO– vs MDTO+,  $A\beta+$  vs  $A\beta-$ ) as a between-subjects factor, and age and sex as covariates of no interest. Main effects and interactions were considered significant at  $p < 0.05$  (two-tailed). We tested for main effects of performance/ $A\beta$  status to determine whether FC was overall different between groups, and significant performance/ $A\beta$  status by FC pair interactions to determine whether groups varied in FC between specific ROI pairs. Main effects and interactions were considered significant at  $p < 0.05$  (two-tailed). In cases of significant group by FC pair interactions, we further examined which ROI pairs were driving this interaction with planned follow-up pairwise comparisons, which were considered significant at  $p < 0.05$  (two-tailed).

Bivariate and partial (controlling for age and sex) correlations were performed to assess relationships between continuous variables. Linear regressions were performed to test interactions between MDTO performance and neurodegeneration in predicting FC, including age and sex in the model. Independent-samples  $t$  tests (two-tailed) were performed to assess group differences in neurodegeneration.

## Results

### Participants

We analyzed resting state fMRI data, structural MRI data, and  $^{18}\text{F}$ -florbetapir PET  $A\beta$  scans from a total of 64 cognitively normal older adults recruited from a community-based sample. Participants completed a comprehensive cognitive assessment

**Table 1. Demographic information and characteristics of the sample**

	<i>N</i>	Mean (SD) or <i>n</i> (%)
Age (years)	64	71.3 (6.4)
Sex (female)	64	43 (67.2%)
Education (years)	64	16.3 (2.3)
MMSE	63	28.5 (1.3)
RAVLT delayed recall	63	10.9 (3.3)
MDTO LDI (high similarity)	56	0.20 (0.13)
MDTS LDI (high similarity)	59	0.20 (0.14)
$A\beta+$	57	19 (33.3%)
Global FBP SUVR	57	1.11 (0.19)

All 64 participants underwent high-resolution resting state fMRI, while subsets additionally underwent  $^{18}\text{F}$ -FBP-PET and performed the mnemonic discrimination task (MDT) LDI was calculated on the high-similarity stimuli.

battery including word list recall as well as the object and spatial mnemonic discrimination tasks. Full demographic information for the sample is included in Table 1.

### Mnemonic discrimination performance and classification

Participants performed object ( $n = 56$ ) and spatial ( $n = 59$ ) versions of the MDT (Fig. 1A). Full descriptions of the tasks are included in Materials and Methods. Briefly, participants first completed a study phase in which they were exposed to the target stimuli. In the test phase, participants judged whether stimuli were target or lure stimuli. In the object task (i.e., MDTO), lure stimuli consist of subtle changes to the object itself, while in the spatial task (i.e., MDTS), lure stimuli consist of changes in the location of the object on a grid. Each lure stimulus can be classified as being of low or high similarity to the original target stimulus. We focused on performance for the highly similar lure stimuli based on our prior work showing that pattern separation mechanisms in older adults are especially impaired for highly similar compared with less similar lures (Yassa et al., 2011a). Performance was measured with the well established LDI [ $p$  (“New or Different” | Lure) –  $p$  (“New or Different” | Target)], which corrects for potential response bias.

Performance on the object and spatial versions of the MDT were moderately correlated ( $r = 0.46$ ,  $p < 0.001$ ), and did not significantly differ (paired-samples  $t$  test,  $t_{(54)} = 0.34$ ,  $p = 0.73$ ). There was no significant association between either object or spatial MDT with age or global FBP SUVR ( $p$  values  $> 0.18$ ) or sex difference in object MDT ( $p = 0.53$ ). However, female participants performed significantly higher than males on the spatial MDT ( $t_{(57)} = 2.13$ ,  $p = 0.04$ ).

We classified participants as either low or high performers on the object and spatial MDT using a median split of the LDI high-similarity score (Fig. 1B; MDTO median = 0.185; MDTS median = 0.21). For the object MDT, 28 participants (50%) were classified as high performers (MDTO+) and 28 participants (50%) were classified as low performers (MDTO–). For the spatial MDT, 26 participants (44%) were classified as high performers (MDTS+) and 33 participants (56%) as low performers (MDTS–).

### Entorhinal–hippocampal circuit functional connectivity

The primary aim of our study was to test how object and spatial mnemonic discrimination was related to FC between regions that comprise the canonical entorhinal–hippocampal circuit (entorhinal subregions and hippocampal subfields). We further investigated whether object and spatial mnemonic discrimination was related to FC between regions contained within the anterior-temporal and posterior-medial cortical networks (Ranganath and

Ritchey, 2012), respectively. This was achieved by analyzing high-resolution (1.8 mm<sup>3</sup>; partial brain acquisition) resting state fMRI data with a highly detailed atlas of ROIs spanning the medial temporal lobe and hippocampus, which are shown in Figure 2A. We conducted ROI-to-ROI FC analyses using the CONN toolbox (Whitfield-Gabrieli and Nieto-Castanon, 2012). To ensure spatial specificity, BOLD time series were extracted from unsmoothed data. Further, we performed semipartial correlations between time series, which controls for signal from all other included ROIs, to mitigate any potential signal bleed in from neighboring regions and to obtain FC values representing the unique FC between regions (Adams et al., 2019; Dalton et al., 2019).

Group-level patterns of FC are shown in Figure 2B. Overall, FC between the two hemispheres was largely consistent, and was strongest within each network (hippocampus, anterior-temporal, and posterior-medial networks). Within the hippocampus, there was strong FC between DG/CA3 and CA1, and between CA1 and Sub, mirroring the known anatomic connectivity of this circuit. Because we did not have hypotheses regarding lateralized hemispheric effects, and to reduce the number of statistical tests, we averaged FC values between left and right hemisphere region pairs before subsequent analyses.

### Impaired object mnemonic discrimination is related to aLEC–DG/CA3 hyperconnectivity

We first tested whether object and spatial mnemonic discrimination was associated with FC within the entorhinal–hippocampal circuit. We focused on FC between region pairs that compose the canonical entorhinal–hippocampal circuit, as follows: aLEC to DG/CA3, pmEC to DG/CA3, DG/CA3 to CA1, and CA1 to Sub. While we acknowledge that FC is a nondirectional measure and structural connectivity does not definitively drive FC, projections within the trisynaptic circuit are likely partially driving these FC measures (Amaral and Lavenex, 2006; Witter, 2007). Primary analyses focused on subfields within the hippocampal head because of the increased vulnerability of this segment to aging and AD (Das et al., 2013; Gordon et al., 2013). We conducted two repeated-measures ANCOVAs, one for each task, with FC pair (aLEC–DG/CA3H; pmEC–DG/CA3H; DG/CA3H–CA1H; CA1H–SubH) as a within-subjects factor, performance (high vs low performers) as a between-subjects factor, and age and sex as covariates of no interest. Our effects of interest were the main effect of performance, indicating that FC differed between the low-performing and high-performing groups uniformly across the circuit, and a performance by FC pair interaction, indicating that FC differed between the low-performing and high-performing groups in specific connections.

We first compared entorhinal–hippocampal circuit FC between low and high performers on the object mnemonic discrimination task (Fig. 3A). While there was no main effect of performance ( $F_{(1)} = 2.27, p = 0.14$ ), we found a significant performance by FC pair interaction ( $F_{(3)} = 3.35, p = 0.02$ ), indicating the low-performing and high-performing groups differed in FC in particular connections within the circuit. Follow-up pairwise comparisons indicated that this interaction was driven by low performers having significantly increased FC between aLEC and DG/CA3H compared to high performers ( $t_{(52)} = 2.81, p = 0.007$ ). There were no other significant performance differences across the circuit ( $p$  values  $> 0.30$ ). The specificity of this result supports our hypothesis that the connection between aLEC and DG/CA3H supports object mnemonic discrimination and its integrity tracks with performance.

We next compared entorhinal–hippocampal FC between low and high performers on the spatial mnemonic discrimination task (Fig. 3B). We did not observe a significant main effect of performance ( $F_{(1)} = 0.81, p = 0.37$ ) or performance by FC pair interaction ( $F_{(3)} = 1.01, p = 0.39$ ), indicating that there were no general or regionally specific differences in entorhinal–hippocampal circuit FC related to spatial mnemonic discrimination performance. However, a targeted analysis of the connection between pmEC and DG/CA3H, which we specifically hypothesized would be related to spatial mnemonic discrimination, identified a trend in which the low performers had decreased FC compared to high performers ( $t_{(55)} = -2.0, p = 0.051$ ).

We then examined whether these effects generalized to the hippocampal tail. We conducted similar ANCOVA models, instead including FC between entorhinal subregions and hippocampal tail ROIs (aLEC–DG/CA3T, pmEC–DG/CA3T, DG/CA3T–CA1T, CA1T–SubT). We found no significant main effect or interaction for the hippocampal tail for either object (main effect of performance:  $F_{(1)} = 0.72, p = 0.40$ ; performance by FC pair interaction:  $F_{(3)} = 1.38, p = 0.25$ ) or spatial (main effect of performance:  $F_{(1)} = 1.20, p = 0.28$ ; performance by FC pair interaction:  $F_{(3)} = 0.37, p = 0.78$ ) mnemonic discrimination performance, suggesting the increase in FC between aLEC and DG/CA3 in the low object mnemonic discrimination group was specific to the hippocampal head.

As a control analysis, we examined whether a general episodic memory performance, rather than mnemonic discrimination, would also be related to differences in aLEC–DG/CA3H FC or any other connection within the circuit (Fig. 3D). To test this, we classified participants as low or high performers on the RAVLT delayed recall test using a median split and performed a similar ANCOVA. There was no significant main effect of performance ( $F_{(1)} = 0.46, p = 0.50$ ) or performance by FC pair interaction ( $F_{(3)} = 1.49, p = 0.22$ ) when splitting the groups by delayed recall episodic memory performance, supporting the specificity of aLEC–DG/CA3H connectivity in supporting mnemonic discrimination.

Finally, we examined whether splitting MDT performance based on all lure similarity trial types, rather than focusing on highly similar lure stimuli, would produce consistent results. For object mnemonic discrimination, we still observed a significant performance by FC pair interaction ( $F_{(3)} = 3.39, p = 0.02$ ), again driven by increased FC between aLEC and DG/CA3H in low performers compared to high performers ( $t_{(52)} = 2.07, p = 0.04$ ); however, this difference was less pronounced than when defining low performance only using high-similarity lure stimuli. Again, there were no significant effects when splitting spatial performance using all lure similarity trials (main effect of performance:  $F_{(1)} = 0.005, p = 0.95$ ; performance by FC pair interaction:  $F_{(3)} = 1.27, p = 0.29$ ).

### A $\beta$ is associated with widespread changes in entorhinal–hippocampal circuit FC

Our second study goal was to determine whether Alzheimer's pathology was also associated with changes to entorhinal–hippocampal circuit FC as a potential mechanism leading to mnemonic discrimination impairment. To assess this, we classified participants as A $\beta$ – ( $n = 38$ ) or A $\beta$ + ( $n = 19$ ) using a threshold of global FBP SUVR  $> 1.11$  (Fig. 1B; Landau et al., 2012). While we did not have a direct measure of tau pathology, older adults classified as A $\beta$ + are highly likely to have tau pathology within the entorhinal cortex (Braak and Braak, 1997). We then conducted repeated-measures ANCOVAs, including FC pair (aLEC–DG/CA3H, pmEC–DG/CA3H, DG/CA3H–CA1H,



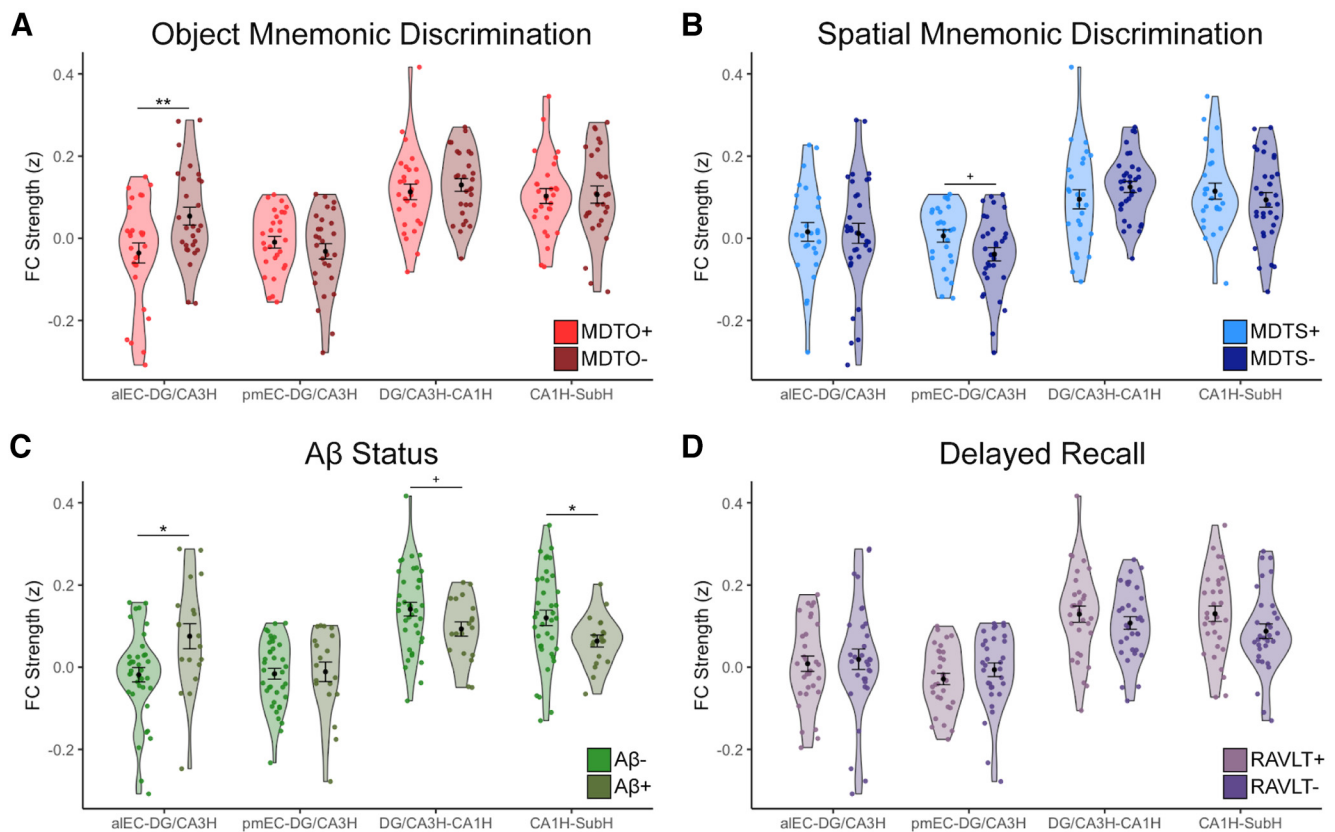


**Figure 3.** Entorhinal–hippocampal functional connectivity (FC) is related to object mnemonic discrimination and  $A\beta$  status. FC strength (Fisher z-transformed semipartial correlation values) was calculated between each region pair corresponding to canonical anatomical connections within the entorhinal–hippocampal circuit. **A**, FC strength was compared between high (MDTO+, light red) and low (MDTO–, dark red) performers on the MDTO. Low performers had significantly increased FC between aIEC and DG/CA3H compared with high performers, but no other differences across the circuit. **B**, FC strength was compared between high (MDTS+, light blue) and low (MDTS–, dark blue) performers on the MDTs. There were no significant differences in FC strength; however, there was a trend-level association for decreased pmEC–DG/CA3H FC in the low performers compared with high performers. **C**, FC strength was compared between  $A\beta$ – (light green) and  $A\beta$ + (dark green) participants.  $A\beta$ + participants had significantly increased FC between aIEC and DG/CA3H compared with  $A\beta$ – participants, which is consistent with the pattern found in the MDTO– group.  $A\beta$ + participants also had decreased FC between CA1H and SubH, and a trend-level association for decreased FC between DG/CA3H and CA1H compared  $A\beta$ – participants. **D**, Control analyses tested whether performance on a traditional episodic memory measure, the RAVLT delayed recall, was associated with changes in entorhinal–hippocampal FC. There was no difference in FC between high (RAVLT+, light purple) and low (RAVLT–, dark purple) performers, indicating specific effects for mnemonic discrimination. Error bars represent the SEM. \*\* $p < 0.01$ , \* $p < 0.05$ , + $p < 0.10$ .

CA1H–SubH) as a within-subjects measure,  $A\beta$  status (positive vs negative) as a between-subjects factor, and age and sex as covariates of no interest, again with either a main effect of  $A\beta$  status or  $A\beta$  status by FC pair interaction as the effects of interest.

While there was no main effect of  $A\beta$  status ( $F_{(1)} = 0.05$ ,  $p = 0.82$ ), we found a significant  $A\beta$  status by FC pair interaction ( $F_{(3)} = 5.73$ ,  $p < 0.001$ ), indicating that  $A\beta$ – and  $A\beta$ + groups differed in FC in particular connections within the circuit (Fig. 3C). Follow-up pairwise comparisons indicated that this interaction was driven by widespread differences across the circuit.  $A\beta$ + participants had significantly increased FC between aIEC and DG/CA3H compared to  $A\beta$ – participants ( $t_{(53)} = -2.67$ ,  $p = 0.01$ ). This increase in aIEC–DG/CA3H FC in the  $A\beta$ + participants mirrors the hyperconnectivity found in the low-object mnemonic discrimination performers. Further,  $A\beta$ + participants had decreased FC between hippocampal subfields.  $A\beta$ + participants had significantly decreased FC between CA1H and SubH compared to the  $A\beta$ – participants ( $t_{(53)} = 2.21$ ,  $p = 0.03$ ), and a trend toward decreased FC between DG/CA3H and CA1H ( $t_{(53)} = 1.71$ ,  $p = 0.09$ ).

We next tested the effect of  $A\beta$  on FC between the entorhinal subregions and subfields within the hippocampal tail. While

there was no significant main effect of  $A\beta$  status ( $F_{(1)} = 0.07$ ,  $p = 0.80$ ), there was a trend for an  $A\beta$  status by FC pair interaction ( $F_{(3)} = 2.48$ ,  $p = 0.06$ ); however, because this effect did not reach statistical significance, we did not conduct follow-up pairwise comparisons.

#### Contributions of anterior-temporal and posterior-medial cortical networks

Because the anterior-temporal network preferentially supports object processing, while the posterior-medial network preferentially supports spatial processing (Ranganath and Ritchey, 2012), we investigated whether FC within these networks was related to object and spatial mnemonic discrimination, respectively. We included aIEC, PRC, and amygdala to represent the anterior-temporal network, and pmEC, parahippocampal gyrus (PHG), and retrosplenial cortex (RSC) to represent the posterior-medial network. We acknowledge that additional regions are commonly included within these networks (Ranganath and Ritchey, 2012); however, we chose to only include ROIs contained within our study-specific template and were somewhat restricted in cortical coverage given our partial field of view from high-resolution scans.



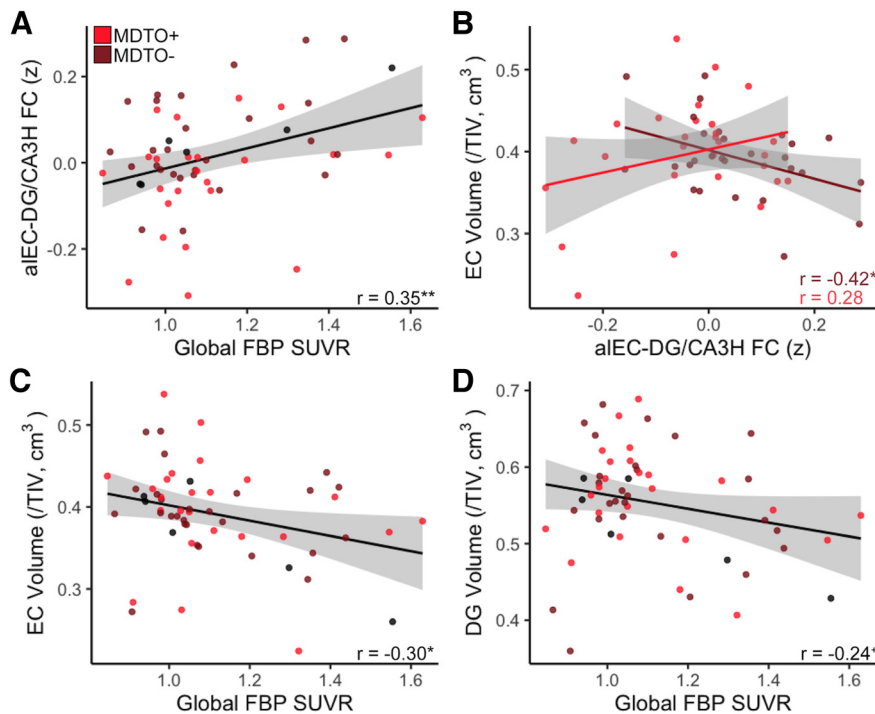


**Figure 4.** Associations between aLEC and DG/CA3H hyperconnectivity with  $A\beta$  and neurodegeneration. **A**, Increased aLEC–DG/CA3H FC was significantly associated with continuous levels of global  $A\beta$  pathology (FBP SUVR). **B**, There was a significant interaction between object mnemonic discrimination performance and neurodegeneration in predicting aLEC–DG/CA3H FC. In the MDTO– group (light red), increased FC between aLEC and DG/CA3H was associated with decreased EC volume, indicating neurodegeneration. There was no significant relationship in the MDTO+ group (dark red). **C**, Increased global FBP SUVR, indicating higher levels of  $A\beta$  pathology, was associated with reduced EC volume. **D**, Increased global FBP SUVR had a trend-level association with reduced DG volume. \*\* $p < 0.01$ , \* $p < 0.05$ , + $p < 0.10$ .

To investigate the relationship between object mnemonic discrimination and the anterior-temporal network, we conducted a repeated-measures ANCOVA with FC pair (aLEC–PRC, aLEC–amyg, PRC–amyg) as a within-subjects measure, performance (high vs low performers) as a between-subjects factor, and age and sex as covariates of no interest. There was no significant main effect of performance ( $F_{(1)} = 0.33$ ,  $p = 0.57$ ) or performance by FC pair interaction ( $F_{(2)} = 0.77$ ,  $p = 0.46$ ), indicating that connectivity between these regions did not strongly contribute to object mnemonic discrimination performance. We conducted a similar repeated-measures ANCOVA for spatial mnemonic discrimination and the posterior-medial network (pmEC–PHG, pmEC–RSC, PHG–RSC). Again, there was no main effect of performance ( $F_{(1)} = 0.38$ ,  $p = 0.54$ ) or performance by FC pair interaction ( $F_{(2)} = 0.21$ ,  $p = 0.81$ ).

Finally, we investigated whether  $A\beta$  positivity was associated with changes in FC within either network, based on evidence that  $A\beta$  accumulates in the posterior-medial network (Maass et al., 2019) and can drive differences in connectivity within these networks (Berron et al., 2020; Cassidy et al., 2021). In the posterior-medial network, while there was no main effect of  $A\beta$  status ( $F_{(1)} = 0.36$ ,  $p = 0.55$ ), there was a significant  $A\beta$  status by FC pair interaction ( $F_{(2)} = 3.99$ ,  $p = 0.02$ ), indicating that FC within this network varied by  $A\beta$  status. *Post hoc* pairwise comparisons indicated that this interaction was driven by the  $A\beta+$  participants having lower FC between pmEC and PHG ( $t_{(53)} = 2.49$ ,  $p = 0.02$ ). Within the anterior-temporal cortical network, there was no significant main effect of  $A\beta$  status ( $F_{(1)} = 2.81$ ,  $p = 0.10$ ) or  $A\beta$  status by FC pair interaction ( $F_{(2)} = 0.22$ ,  $p = 0.80$ ).

### Factors associated with aLEC–DG/CA3H hyperconnectivity

Because of the strong association of increased FC between aLEC and DG/CA3 with both low object mnemonic discrimination performance and  $A\beta$  positivity, we conducted follow-up analyses to further explore factors related to this hyperconnectivity. We first examined whether aLEC–DG/CA3H FC was continuously related to both performance on object mnemonic discrimination and levels of  $A\beta$  (global FBP SUVR). While the continuous association between object mnemonic discrimination and aLEC–DG/CA3H FC did not reach significance ( $r = -0.19$ ,  $p = 0.17$ ), we found a strong continuous association between higher global FBP SUVR and increased aLEC–DG/CA3H FC ( $r = 0.35$ ,  $p = 0.008$ ; Fig. 4A), which remained significant when controlling for age and sex ( $r = 0.34$ ,  $p = 0.01$ ).

We next investigated whether aLEC–DG/CA3H hyperconnectivity was related to neurodegeneration in these regions. To test this, we calculated native-space volume estimates using ASHS software, corrected for total intracranial volume (see Materials and Methods). Because ASHS segmentation does not provide separate estimates for aLEC and pmEC or for hippocampal head versus tail, we used the total volume of EC, DG, and CA3 in our analyses. Across all participants, there was

no significant relationship between aLEC–DG/CA3H FC and the volume of these regions (EC:  $r = -0.09$ ,  $p = 0.49$ ; DG:  $r = -0.14$ ,  $p = 0.29$ ; CA3:  $r = -0.16$ ,  $p = 0.21$ ). However, we found a significant interaction between object mnemonic discrimination performance and EC volume in predicting aLEC–DG/CA3H FC (model:  $F_{(50)} = 3.04$ ,  $p = 0.02$ ; interaction:  $t = 2.51$ ,  $p = 0.02$ ; Fig. 4B). Investigating this interaction further, we found that within the low object mnemonic discrimination group, increased aLEC–DG/CA3H FC was related to decreased EC volume ( $r = -0.42$ ,  $p = 0.03$ ; controlling for age and sex:  $r = -0.38$ ,  $p = 0.06$ ), while there was no significant relationship in the high object mnemonic discrimination group ( $r = 0.28$ ,  $p = 0.15$ ). This interaction was specific to EC volume; we did not observe a similar effect with DG or CA3 volume (model  $p$  values  $> 0.10$ ; interaction  $p$  values  $> 0.30$ ). Finally, performance on the object mnemonic discrimination task (both continuous associations and group comparisons) was not directly associated with volume in EC, DG, or CA3 ( $p$  values  $> 0.55$ ).

Because  $A\beta$  pathology was also related to aLEC–DG/CA3 hyperconnectivity, we next tested whether  $A\beta$  was associated with neurodegeneration in these regions. Comparing the volume of these regions in  $A\beta+$  and  $A\beta-$  groups indicated that  $A\beta+$  older adults had reduced volume in both EC ( $t_{(55)} = 2.44$ ,  $p = 0.02$ ) and DG ( $t_{(55)} = 2.97$ ,  $p = 0.004$ ), but not CA3 ( $t_{(55)} = 0.58$ ,  $p = 0.56$ ). Further, a higher level of global FBP SUVR was associated with decreased volume in EC ( $r = -0.30$ ,  $p = 0.03$ ; controlling for age and sex:  $r = -0.27$ ,  $p = 0.04$ ; Fig. 4C), with a trend for decreased volume in DG ( $r = -0.24$ ,  $p = 0.08$ ; controlling for age and sex:  $r = -0.22$ ,  $p = 0.11$ ; Fig. 4D) and no

significant relationship in CA3 ( $r = -0.08$ ,  $p = 0.56$ ). Together, these results indicate that the volume of the entorhinal cortex is closely associated with increased FC between aEC–DG/CA3H in low-object mnemonic discrimination performers as well as  $A\beta$  pathology.

### Factors associated with CA1H–SubH hypoconnectivity

Because FC between CA1H and SubH was found to be decreased in  $A\beta^+$  older adults, we also explored how levels of  $A\beta$  and neurodegeneration were related to this hypoconnectivity. We found trend-level associations between decreased CA1H–SubH FC and both higher global FBP SUVR ( $r = -0.25$ ,  $p = 0.06$ ; controlling for age and sex:  $r = -0.26$ ,  $p = 0.052$ ; Fig. 5A) and decreased CA1 volume ( $r = 0.22$ ,  $p = 0.09$ ; controlling for age and sex:  $r = 0.22$ ,  $p = 0.08$ ; Fig. 5B), but no relationship with Sub volume ( $r = 0.09$ ,  $p = 0.50$ ; controlling for age and sex:  $r = 0.08$ ,  $p = 0.52$ ).

Next, we investigated relationships between  $A\beta$  pathology and neurodegeneration in CA1 and Sub.  $A\beta^+$  older adults had reduced volume in CA1 ( $t_{(55)} = 3.05$ ,  $p = 0.004$ ) and Sub ( $t_{(55)} = 3.02$ ,  $p = 0.004$ ) compared with  $A\beta^-$  older adults. Further, higher global FBP SUVR was continuously associated with decreased volume in CA1 ( $r = -0.28$ ,  $p = 0.03$ ; controlling for age and sex:  $r = -0.29$ ,  $p = 0.03$ ; Fig. 5C) and Sub ( $r = -0.31$ ,  $p = 0.02$ ; controlling for age and sex:  $r = -0.34$ ,  $p = 0.01$ ; Fig. 5D). These results suggest strong relationships between  $A\beta$  pathology and the volume of both CA1 and Sub.

### Discussion

Our results provide evidence that the integrity of communication within the entorhinal–hippocampal circuit, measured with resting state FC, is related to mnemonic discrimination performance and  $A\beta$  pathology in cognitively normal older adults. We demonstrate that hyperconnectivity between aEC and DG/CA3 is related to both poor object mnemonic discrimination performance and  $A\beta$  pathology. Increased FC in low-object mnemonic discrimination performers was also associated with neurodegeneration within entorhinal cortex, but not DG or CA3, suggesting that entorhinal dysfunction may primarily drive hyperconnectivity. There were no significant FC differences underlying spatial mnemonic discrimination, suggesting that spatial memory deficits may not be as prevalent in cognitively normal older adults at this stage. Further,  $A\beta$  pathology was associated with hypoconnectivity between CA1 and Sub, as well as decreased volume within these regions, suggesting that  $A\beta$  has widespread effects on the integrity of the entorhinal–hippocampal circuit. Together, our findings indicate that specific alterations in communication between aEC and DG/CA3 contribute to the vulnerability of object mnemonic discrimination in aging, which may be attributable to underlying Alzheimer's pathology.

To our knowledge, our study is the first examination of high-resolution resting state FC between entorhinal subregions and

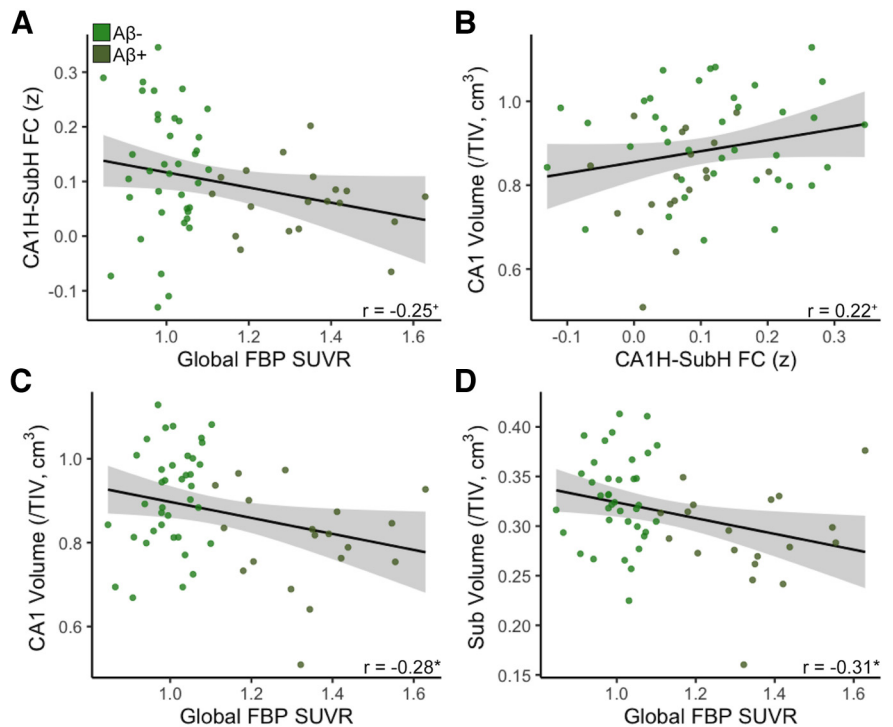


**Figure 5.** Associations between CA1H and SubH hypoconnectivity with  $A\beta$  and neurodegeneration. **A**, There was a trend-level association between decreased CA1H–SubH FC with increased levels of global  $A\beta$  pathology (FBP SUVR). **B**, There was a trend-level association between decreased CA1H–SubH FC and CA1 volume. **C**, Increased FBP SUVR was significantly associated with reduced CA1 volume. **D**, Increased FBP SUVR was significantly associated with reduced Sub volume. \* $p < 0.05$ , + $p < 0.10$ .

hippocampal subfields with mnemonic discrimination in cognitively normal older adults. We demonstrate that object mnemonic discrimination performance was specifically related to hyperconnectivity between aEC and DG/CA3, particularly within the hippocampal head. This finding supports both human and animal data showing that the perforant path connecting entorhinal cortex and dentate gyrus is essential for mnemonic discrimination (Yassa et al., 2011a; Bennett and Stark, 2016; Burke et al., 2018). We extend previous findings by showing that object mnemonic discrimination performance is localized to connectivity between DG/CA3 and aEC, rather than pmEC, which is consistent with models of distinct processing streams in entorhinal cortex (Maass et al., 2015). The specificity of aEC–DG/CA3 FC for mnemonic discrimination is further supported by our control analysis demonstrating that this connection was not associated with performance on a delayed recall measure of episodic memory. While input from the entorhinal cortex to the hippocampus is critical for all hippocampal function (Witter, 2007), subtle changes in this connection may first emerge as mnemonic discrimination deficits that can be observed while older adults are still cognitively normal. This further supports the notion that mnemonic discrimination performance is a highly sensitive marker of emerging cognitive decline.

Our findings extend previous task-based fMRI findings investigating medial temporal lobe activation during mnemonic discrimination in aging (Marks et al., 2017; Reagh et al., 2018; Berron, 2019; Tran et al., 2021). One study showed impaired object mnemonic discrimination in older adults was associated with relative hypoactivity within aEC and hyperactivity within DG/CA3 compared to young adults (Reagh et al., 2018). Hypoactivation in aEC was correlated with DG/CA3 hyperactivation, suggesting a

functional link between the two processes. We interpret our finding of increased aEC–DG/CA3 FC to reflect coordinated hyperactivation in the entorhinal–hippocampal circuit at rest, while aEC hypoactivation may emerge during active mnemonic discrimination processing when analyzing specific contrasts or group comparisons (Reagh et al., 2018; Tran et al., 2021).

Because increased FC was associated with  $A\beta$  pathology and neurodegeneration, it suggests that this hyperconnectivity is dysfunctional rather than compensatory. A pathological increase in FC between the entorhinal cortex and hippocampus at rest is supported by previous work (Das et al., 2013; Sinha et al., 2019; Berron et al., 2020; Dautricourt et al., 2021). For example, studies comparing resting state FC between mild cognitive impairment/AD patients and elderly control subjects have found increased FC between entorhinal cortex and hippocampus, particularly with the hippocampal head (Das et al., 2013), which is consistent with our results. Another study found increased FC between the entorhinal cortex and hippocampal subfields in healthy older African Americans at genetic risk for AD, which was associated with impaired ability to generalize previously learned information (Sinha et al., 2019).

Our study provides novel evidence that hyperconnectivity between the entorhinal cortex and DG/CA3 is related to  $A\beta$  pathology. Findings from animal models suggest that  $A\beta$  increases neural synchrony and elicits epileptiform activity (Busche et al., 2008; Palop and Mucke, 2010), which may express as increased resting state FC. Supporting these findings from animal models, in human neuroimaging studies  $A\beta$  pathology is associated with hyperactivation in both the hippocampus and entorhinal cortex (Mormino et al., 2012; Huijbers et al., 2014, 2015) and hyperconnectivity between cortical networks (Schultz et al., 2017).  $A\beta$  may also indirectly lead to hyperconnectivity by promoting development of tau in the entorhinal cortex (Sanchez et al., 2021; Adams et al., 2022), which is associated with hyperactivity in medial temporal lobe (Huijbers et al., 2019; Maass et al., 2019; Adams et al., 2021). Together, these findings in combination with our current results suggest that the hyperconnectivity between aEC and DG/CA3 may be a result of Alzheimer's pathology, which preferentially disrupts aEC–DG/CA3 communication and expresses as impaired object mnemonic discrimination.

We did not observe any statistically significant relationships between spatial mnemonic discrimination performance and entorhinal–hippocampal circuit FC. This is consistent with previous studies in cognitively normal older adults that failed to find relationships between spatial mnemonic discrimination and abnormal task-based activation in pmEC (Reagh et al., 2018; Berron, 2019) or deficits in performance (Reagh et al., 2018) compared with young adults. However, a targeted analysis of the hypothesized connection between pmEC, which preferentially supports spatial processing (Maass et al., 2015), and DG/CA3H revealed a nearly significant difference between high-performing and low-performing groups. It is likely that the connection between pmEC and DG/CA3, as well as performance on spatial mnemonic discrimination, is affected later in the development of AD.

$A\beta$  pathology was also related to further hypoconnectivity and neurodegeneration within the hippocampus itself, particularly involving CA1 and Sub. Hypoconnectivity within the hippocampus may be a direct result of hyperconnectivity between entorhinal cortex and hippocampus. A study in mice found that  $A\beta$ -related excitatory increases in entorhinal cortex activation were associated with compensatory downregulation of subiculum activity, which was proposed to be a protective response (Angulo

et al., 2017). The connection between CA1 and Sub is of particular interest due to the propensity of tau pathology to target these subfields while sparing DG/CA3 until late stages of AD (Braak and Braak, 1991). Future research should investigate specific tasks that probe CA1 and Sub in the context of aging and preclinical AD to determine whether FC between these regions is associated with cognitive performance.

We did not find contributions of anterior-temporal and posterior-medial cortical networks to object or spatial mnemonic discrimination performance, respectively. Previous work has demonstrated a loss of functional specificity within these networks in aging (Berron et al., 2018; Maass et al., 2019). Because of our high-resolution sequence with partial field of view focused on medial temporal lobe, we were unable to sample certain cortical regions commonly considered parts of these networks (Ranganath and Ritchey, 2012). Disrupted FC in these networks may arise later in disease progression or contribute more broadly to memory than specific deficits in mnemonic discrimination. Nonetheless,  $A\beta$  was associated with FC within the posteromedial network, which is consistent with previous findings (Maass et al., 2019; Cassidy et al., 2021).

There was no direct association between mnemonic discrimination performance and neurodegeneration. This suggests that FC, which can reflect both coordinated activation and structural connections, may be more sensitive to subtle cognitive changes. Previous studies have identified relationships between aEC volume/thickness and cognition in older adults (Olsen et al., 2017; Holbrook et al., 2019; Tran et al., 2021). However, because changes in neural function occur before overt neurodegeneration, it is likely that our results are detecting dysfunction that may not yet be observable with coarse structural measurements such as volume.

This study has several limitations. First, we did not have tau-PET to evaluate tau within medial temporal lobe. While  $A\beta+$  participants are highly likely to have entorhinal tau pathology (Braak and Braak, 1997), some participants classified as  $A\beta-$  may also have age-related development of tau in medial temporal lobe (Crary et al., 2014). Previous work in cognitively normal older adults has shown that the medial temporal tau-PET signal is related to lure discrimination on an emotional pattern separation task, but only within  $A\beta+$  participants (Leal et al., 2019), which suggests that  $A\beta$  may potentiate the effects of tau pathology on memory. Second, different ROIs were used to calculate volume than the ROIs used to calculate FC, which may have diminished the strength of associations due the decreased specificity of the regions. Nonetheless, we observed associations between volume with both FC and  $A\beta$  pathology. Finally, 7T fMRI data could enable an even more precise measurement of FC within subfield ROIs (Berron et al., 2016). However, we applied semipartial correlations and no spatial smoothing to control for potential blurring of signal from adjacent ROIs and found distinct patterns of FC that matched our hypotheses and previous literature. Replication of our findings at higher resolution may uncover additional novel associations.

In conclusion, our results suggest that  $A\beta$  pathology indirectly leads to mnemonic discrimination impairment through entorhinal–hippocampal circuit dysfunction. The vulnerability of the aEC to Alzheimer's pathology may result in altered communication with DG/CA3, leading to impairment of object mnemonic discrimination early in the pathogenesis of AD.  $A\beta$  pathology further contributes to altered FC and neurodegeneration within the hippocampus itself, indicating more general dysfunction. Because resting state FC is easier to acquire than



task-based fMRI, several existing large-scale studies have worked to harmonize sequences across sites. However, more work is still needed to establish the foundational principles related to the use of these data in clinical trials. That said, disruptions in FC within the entorhinal–hippocampal circuit could be a promising biomarker of emerging memory decline.

## References

- Adams JN, Maass A, Harrison TM, Baker SL, Jagust WJ (2019) Cortical tau deposition follows patterns of entorhinal functional connectivity in aging. *Elife* 8:e49132.
- Adams JN, Maass A, Berron D, Harrison TM, Baker SL, Thomas WP, Stanfill M, Jagust WJ (2021) Reduced repetition suppression in aging is driven by tau-related hyperactivity in medial temporal lobe. *J Neurosci* 41:3917–3931.
- Adams JN, Harrison TM, Maass A, Baker SL, Jagust WJ (2022) Distinct factors drive the spatiotemporal progression of tau pathology in older adults. *J Neurosci* 42:1352–1361.
- Amaral DG, Lavenex P (2006) Hippocampal neuroanatomy. In: *The hippocampus book* (Andersen P, Morris R, Amaral D, Bliss T, O'Keefe J, eds). Oxford: Oxford UP.
- Angulo SL, Orman R, Neymotin SA, Liu L, Buitrago L, Cepeda-Prado E, Stefanov D, Lytton WW, Stewart M, Small SA, Duff KE, Moreno H (2017) Tau and amyloid-related pathologies in the entorhinal cortex have divergent effects in the hippocampal circuit. *Neurobiol Dis* 108:261–276.
- Bakker A, Krauss GL, Albert MS, Speck CL, Jones LR, Stark CE, Yassa MA, Bassett SS, Shelton AL, Gallagher M (2012) Reduction of hippocampal hyperactivity improves cognition in amnesic mild cognitive impairment. *Neuron* 74:467–474.
- Behzadi Y, Restom K, Liu J, Liu TT (2007) A component based noise correction method (CompCor) for BOLD and perfusion based fMRI. *Neuroimage* 37:90–101.
- Bennett IJ, Stark CEL (2016) Mnemonic discrimination relates to perforant path integrity: an ultra-high resolution diffusion tensor imaging study. *Neurobiol Learn Mem* 129:107–112.
- Berron D, Schütze H, Maass A, Cardenas-Blanco A, Kuijff HJ, Kumaran D, Düzel E (2016) Strong evidence for pattern separation in human dentate gyrus. *J Neurosci* 36:7569–7579.
- Berron D, Neumann K, Maass A, Schütze H, Fließbach K, Kiven V, Jessen F, Sauvage M, Kumaran D, Düzel E (2018) Age-related functional changes in domain-specific medial temporal lobe pathways. *Neurobiol Aging* 65:86–97.
- Berron D, Cardenas-Blanco A, Bittner D, Metzger CD, Spottke A, Heneka MT, Fließbach K, Schneider A, Teipel SJ, Wagner M, Speck O, Jessen F, Düzel E (2019) Higher CSF tau levels are related to hippocampal hyperactivity and object mnemonic discrimination in older adults. *J Neurosci* 39:8788–8797.
- Berron D, van Westen D, Ossenkoppele R, Strandberg O, Hansson O (2020) Medial temporal lobe connectivity and its associations with cognition in early Alzheimer's disease. *Brain* 143:1233–1248.
- Braak H, Braak E (1985) On areas of transition between entorhinal allocortex and temporal isocortex in the human brain. Normal morphology and lamina-specific pathology in Alzheimer's disease. *Acta Neuropathol* 68:325–332.
- Braak H, Braak E (1991) Neuropathological staging of Alzheimer-related changes. *Acta Neuropathol* 82:239–259.
- Braak H, Braak E (1997) Frequency of stages of Alzheimer-related lesions in different age categories. *Neurobiol Aging* 18:351–357.
- Burke SN, Turner SM, Desrosiers CL, Johnson SA, Maurer AP (2018) Perforant path fiber loss results in mnemonic discrimination task deficits in young rats. *Front Syst Neurosci* 12:61.
- Busche MA, Eichhoff G, Adelsberger H, Abramowski D, Wiederhold K, Haass C, Staufenberg M, Konnerth A, Garaschuk O (2008) Clusters of hyperactive neurons near amyloid plaques in a mouse model of Alzheimer's Disease. *Science* 321:1686–1689.
- Cassady KE, Adams JN, Chen X, Maass A, Harrison TM, Landau S, Baker S, Jagust W (2021) Alzheimer's pathology is associated with dedifferentiation of intrinsic functional memory networks in aging. *Cereb Cortex* 31:4781–4793.
- Crary JF, et al. (2014) Primary age-related tauopathy (PART): a common pathology associated with human aging. *Acta Neuropathol* 128:755–766.
- Dalton MA, McCormick C, De Luca F, Clark IA, Maguire EA (2019) Functional connectivity along the anterior–posterior axis of hippocampal subfields in the ageing human brain. *Hippocampus* 29:1049–1062.
- Das SR, Pluta J, Mancuso L, Kliot D, Orozco S, Dickerson BC, Yushkevich PA, Wolk DA (2013) Increased functional connectivity within medial temporal lobe in mild cognitive impairment. *Hippocampus* 23:1–6.
- Dautricourt S, de Flores R, Landeau B, Poinsel G, Vanhoutte M, Delcroix N, Eustache F, Vivien D, de la Sayette V, Chételat G (2021) Longitudinal changes in hippocampal network connectivity in Alzheimer's disease. *Ann Neurol* 90:391–406.
- Fischl B (2012) FreeSurfer. *Neuroimage* 62:774–781.
- Folstein MF, Folstein SE, McHugh PR (1975) "Mini-mental state": a practical method for grading the cognitive state of patients for the clinician. *J Psychiatr Res* 12:189–198.
- Gallagher M, Bizon JL, Hoyt EC, Helm KA, Lund PK (2003) Effects of aging on the hippocampal formation in a naturally occurring animal model of mild cognitive impairment. *Exp Gerontol* 38:71–77.
- Gallagher M, Colantuoni C, Eichenbaum H, Haberman RP, Rapp PR, Tanila H, Wilson IA (2006) Individual differences in neurocognitive aging of the medial temporal lobe. *Age (Dordr)* 28:221–233.
- Gordon BA, Blazey T, Benzinger TLS, Head D (2013) Effects of aging and Alzheimer's disease along the longitudinal axis of the hippocampus. *J Alzheimers Dis* 37:41–50.
- Güsten J, Ziegler G, Düzel E, Berron D (2021) Age impairs mnemonic discrimination of objects more than scenes: a web-based, large-scale approach across the lifespan. *Cortex* 137:138–148.
- Holbrook A, Tustison N, Marquez F, Roberts J, Michael A (2019) Anterolateral entorhinal cortex thickness as a new biomarker for early detection of Alzheimer's disease. *Alzheimers Dement (Amst)* 12:e12068.
- Huijbers W, Mormino EC, Wigman SE, Ward AM, Vannini P, McLaren DG, Becker JA, Schultz AP, Hedden T, Johnson KA, Sperling RA (2014) Amyloid deposition is linked to aberrant entorhinal activity among cognitively normal older adults. *J Neurosci* 34:5200–5210.
- Huijbers W, Mormino EC, Schultz AP, Wigman S, Ward AM, Larvie M, Amariglio RE, Marshall GA, Rentz DM, Johnson KA, Sperling RA (2015) Amyloid- $\beta$  deposition in mild cognitive impairment is associated with increased hippocampal activity, atrophy and clinical progression. *Brain* 138:1023–1035.
- Huijbers XW, Schultz AP, Papp KV, Lapoint MR, Hanseeuw X, Chhatwal XJP, Hedden T, Johnson XA, Sperling XRA (2019) Tau accumulation in clinically normal older adults is associated with hippocampal hyperactivity. *J Neurosci* 39:548–556.
- Insausti R, Juottonen K, Soininen H, Insausti AM, Partanen K, Vainio P, Laakso MP, Pitkänen A (1998) MR volumetric analysis of the human entorhinal, perirhinal, and temporopolar cortices. *Am J Neuroradiol* 19:659–671.
- Jack CR, Knopman DS, Jagust WJ, Shaw LM, Aisen PS, Weiner MW, Petersen RC, Trojanowski JQ (2010) Hypothetical model of dynamic biomarkers of the Alzheimer's pathological cascade. *Lancet Neurol* 9:119–128.
- Knierim JJ, Neunuebel JP, Deshmukh SS (2014) Functional correlates of the lateral and medial entorhinal cortex: objects, path integration and local–global reference frames. *Philos Trans R Soc Lond B Biol Sci* 369:20130369.
- Landau SM, Mintun MA, Joshi AD, Koeppel RA, Petersen RC, Aisen PS, Weiner MW, Jagust WJ (2012) Amyloid deposition, hypometabolism, and longitudinal cognitive decline. *Ann Neurol* 72:578–586.
- Leal SL, Yassa MA (2018) Integrating new findings and examining clinical applications of pattern separation. *Nat Neurosci* 21:163–173.
- Leal SL, Ferguson LA, Harrison TM, Jagust WJ (2019) Development of a mnemonic discrimination task using naturalistic stimuli with applications to aging and preclinical Alzheimer's disease. *Learn Mem* 26:219–228.
- Lemieux L, Salek-Haddadi A, Lund TE, Laufs H, Carmichael D (2007) Modelling large motion events in fMRI studies of patients with epilepsy. *Magn Reson Imaging* 25:894–901.
- Maass A, Berron D, Libby L, Ranganath C, Düzel E (2015) Functional subregions of the human entorhinal cortex. *Elife* 4:e06426.
- Maass A, Berron D, Harrison TM, Adams JN, La Joie R, Baker S, Mellinger T, Bell RK, Swinnerton K, Inglis B, Rabinovici GD, Düzel E, Jagust WJ (2019) Alzheimer's pathology targets distinct memory networks in the ageing brain. *Brain* 142:2492–2509.



- Marks SM, Lockhart SN, Baker SL, Jagust WJ (2017) Tau and  $\beta$ -amyloid are associated with medial temporal lobe structure, function and memory encoding in normal aging. *J Neurosci* 37:3192–3201.
- Mormino EC, Brandel MG, Madison CM, Marks S, Baker SL, Jagust WJ (2012) A $\beta$  deposition in aging is associated with increases in brain activation during successful memory encoding. *Cereb Cortex* 22:1813–1823.
- Navarro Schröder T, Haak KV, Zaragoza Jimenez NI, Beckmann CF, Doeller CF (2015) Functional topography of the human entorhinal cortex. *Elife* 4:e06738.
- Olsen RK, Yeung LK, Noly-Gandon A, D'Angelo MC, Kacollja A, Smith VM, Ryan JD, Barense MD (2017) Human anterolateral entorhinal cortex volumes are associated with cognitive decline in aging prior to clinical diagnosis. *Neurobiol Aging* 57:195–205.
- Palop JJ, Mucke L (2010) Amyloid-beta-induced neuronal dysfunction in Alzheimer's disease: from synapses toward neural networks. *Nat Neurosci* 13:812–818.
- Power JD, Schlaggar BL, Petersen SE (2015) Recent progress and outstanding issues in motion correction in resting state fMRI. *Neuroimage* 105:536–551.
- Ranganath C, Ritchey M (2012) Two cortical systems for memory-guided behaviour. *Nat Rev Neurosci* 13:713–726.
- Reagh ZM, Yassa MA (2014) Object and spatial mnemonic interference differentially engage lateral and medial entorhinal cortex in humans. *Proc Natl Acad Sci U S A* 111:E4264–E4273.
- Reagh ZM, Roberts JM, Ly M, Diprospero N, Murray E, Yassa MA (2014) Spatial discrimination deficits as a function of mnemonic interference in aged adults with and without memory impairment. *Hippocampus* 24:303–314.
- Reagh ZM, Ho HD, Leal SL, Noche JA, Chun A, Murray EA, Yassa MA (2016) Greater loss of object than spatial mnemonic discrimination in aged adults. *Hippocampus* 26:417–422.
- Reagh ZM, Noche JA, Tustison NJ, Delisle D, Murray EA, Yassa MA (2018) Functional imbalance of anterolateral entorhinal cortex and hippocampal dentate/CA3 underlies age-related object pattern separation deficits. *Neuron* 97:1187–1198.e4.
- Rey A (1958) L'examen clinique en psychologie [The clinical examination in psychology]. Paris: Presses Universitaires De France.
- Sanchez JS, Becker JA, Jacobs HIL, Hanseeuw BJ, Jiang S, Schultz AP, Properzi MJ, Katz SR, Beiser A, Satizabal CL, Donnell AO, Decarli C, Quiroz YT, Rentz DM, Sperling RA, Seshadri S (2021) The cortical origin and initial spread of medial temporal tauopathy in Alzheimer's disease assessed with positron emission tomography. *Sci Transl Med* 13:eabc0655.
- Schultz AP, Chhatwal JP, Hedden T, Mormino EC, Hanseeuw BJ, Sepulcre J, Huijbers W, LaPoint M, Buckley RF, Johnson KA, Sperling RA (2017) Phases of hyperconnectivity and hypoconnectivity in the default mode and salience networks track with amyloid and tau in clinically normal individuals. *J Neurosci* 37:4323–4331.
- Sinha N, Reagh ZM, Tustison NJ, Berg CN, Shaw A, Myers CE, Hill D, Yassa MA, Gluck MA (2019) ABCA7 risk variant in healthy older african americans is associated with a functionally isolated entorhinal cortex mediating deficient generalization of prior discrimination training. *Hippocampus* 29:527–538.
- Stark SM, Yassa MA, Stark CEL (2010) Individual differences in spatial pattern separation performance associated with healthy aging in humans. *Learn Mem* 17:284–288.
- Stark SM, Yassa MA, Lacy JW, Stark CEL (2013) A task to assess behavioral pattern separation (BPS) in humans. *Neuropsychologia* 51:2442–2449.
- Tran TT, Speck CL, Gallagher M, Bakker A (2021) Lateral entorhinal cortex dysfunction in amnesic mild cognitive impairment. *Neurobiol Aging* 112:151–160.
- Tustison NJ, Cook PA, Holbrook AJ, Johnson HJ, Muschelli J, Devenyi GA, Duda JT, Das SR, Cullen NC, Gillen DL, Yassa MA, Stone JR, Gee JC, Avants BB (2021) The ANTsX ecosystem for quantitative biological and medical imaging. *Sci Rep* 11:9068.
- Whitfield-Gabrieli S, Nieto-Castanon A (2012) Conn: a functional connectivity toolbox for correlated and anticorrelated brain networks. *Brain Connect* 2:125–141.
- Wilson IA, Ikonen S, Gallagher M, Eichenbaum H, Tanila H (2005) Age-associated alterations of hippocampal place cells are subregion specific. *J Neurosci* 25:6877–6886.
- Wilson IA, Gallagher M, Eichenbaum H, Tanila H (2006) Neurocognitive aging: prior memories hinder new hippocampal encoding. *Trends Neurosci* 29:662–670.
- Wisse LEM, et al. (2017) A harmonized segmentation protocol for hippocampal and parahippocampal subregions: why do we need one and what are the key goals? *Hippocampus* 27:3–11.
- Witter MP (2007) The perforant path: projections from the entorhinal cortex to the dentate gyrus. *Prog Brain Res* 163:43–61.
- Yassa MA, Stark CEL (2011) Pattern separation in the hippocampus. *Trends Neurosci* 34:515–525.
- Yassa MA, Stark SM, Bakker A, Albert MS, Gallagher M, Stark CEL (2010) High-resolution structural and functional MRI of hippocampal CA3 and dentate gyrus in patients with amnesic mild cognitive impairment. *Neuroimage* 51:1242–1252.
- Yassa MA, Mattfeld AT, Stark SM, Stark CEL (2011a) Age-related memory deficits linked to circuit-specific disruptions in the hippocampus. *Proc Natl Acad Sci U S A* 108:8873–8878.
- Yassa MA, Lacy JW, Stark SM, Albert MS, Gallagher M, Stark CEL (2011b) Pattern separation deficits associated with increased hippocampal CA3 and dentate gyrus activity in nondemented older adults. *Hippocampus* 21:968–979.
- Yushkevich PA, Pluta JB, Wang H, Xie L, Ding SL, Gertje EC, Mancuso L, Kliot D, Das SR, Wolk DA (2015) Automated volumetry and regional thickness analysis of hippocampal subfields and medial temporal cortical structures in mild cognitive impairment. *Hum Brain Mapp* 36:258–287.